Cancer Science
Japanese Cancer Association JCA
Open Access

MicroRNA-181b-5p, ETS1, and the c-Met pathway exacerbate the prognosis of pancreatic ductal adenocarcinoma after radiation therapy

Hideo Tomihara,[1] Daisaku Yamada,[1] Hidetoshi Eguchi,[1] Yoshifumi Iwagami,[1] Takehiro Noda,[1] Tadafumi Asaoka,[1] Hiroshi Wada,[1] Koichi Kawamoto,[1] Kunihito Gotoh,[1] Yutaka Takeda,[1,2] Masahiro Tanemura,[1,3] Masaki Mori[1] and Yuichiro Doki[1]

[1]Department of Gastroenterological Surgery, Graduate School of Medicine, Osaka University, Osaka; [2]Department of Surgery, Kansai Rosai Hospital, Hyogo; [3]Department of Surgery, Osaka Police Hospital, Osaka, Japan

Key words

c-Met, ETS1, miR-181b, pancreatic ductal adenocarcinoma, preoperative chemoradiation therapy

Correspondence

Hidetoshi Eguchi, Department of Gastroenterological Surgery, Graduate School of Medicine, Osaka University, 2-2 (E2), Yamadaoka, Suita, Osaka 565-0871, Japan.
Tel: +81-6-6879-3251; Fax: +81-6-6879-3259;
E-mail: heguchi@gesurg.med.osaka-u.ac.jp

Funding Information

Osaka Cancer Society; Pancreas Research Foundation of Japan.

Received August 5, 2016; Revised December 27, 2016; Accepted December 29, 2016

Cancer Sci **108** (2017) 398–407

doi: 10.1111/cas.13159

Preoperative chemoradiation therapy (CRT) for pancreatic ductal adenocarcinoma (PDAC) has emerged as a reasonable strategy that shows good prognostic impact. However, after preoperative CRT, resected specimens show remnant tumor cells, which indicate that some tumor cells had acquired or were selected for resistance to CRT. Recently, two oncological mechanisms, the EMT and the presence of CSCs, were reported to be associated with resistance in various cancers. Previous reports showed that HGF could induce EMT in PDAC cells; moreover, the HGF receptor, c-Met, was identified as a dominant pancreatic CSC marker. However, the clinical significance of c-Met expression remains unclear. So, we hypothesized that remnant PDAC tissue after CRT might harbor cells with high c-Met expression, and these cells may exacerbate patients' prognosis. In the immunohistochemical analysis, we showed that preoperative CRT was significantly associated with high c-Met expression; moreover, high c-Met expression was a significant marker of a dismal prognosis. Next, we investigated mechanisms of c-Met upregulation in PDAC cells. We established GEM-resistant and radioresistant PDAC cells to analyze the transcriptome involved in c-Met expression. The microarray data for the established radiation-resistant PDAC cells indicated miR-181b-5p downregulation, which targets ETS1, one of the transcription factors for c-Met, and it was shown that radiation exposure induced c-Met expression through ETS1 increase by the suppression of miR-181b-5p. These results suggested that targeting these mechanisms may promote the development of a novel multidisciplinary treatment strategy for improving preoperative CRT efficiency.

Pancreatic ductal adenocarcinoma is one of the most lethal diseases worldwide, and its incidence is increasing.[1] Pancreatic ductal adenocarcinoma is the fourth leading cause of cancer deaths, and the National Cancer Institute has estimated that approximately 53 070 new cases and 41 780 deaths occurred in 2016.[2] Pancreatic ductal adenocarcinoma has a dismal 5-year survival rate of 6–8%, which has not improved in the past few decades.[2,3] Although surgical resection remains the only curative treatment option, surgery alone could not provide satisfactory survival rates for patients with PDAC. Thus, various multidisciplinary treatments, including curative surgery, have been developed for treating PDAC. Adjuvant chemotherapy with GEM or fluorouracil-based drugs has significantly prolonged both disease-free and overall survival, and therefore, adjuvant chemotherapy following a curative surgery is now a standard strategy. However, the survival rate remains relatively low; the average 5-year survival rate is 20.7%.[4] To achieve a more preferable prognosis, it is suggested that there is considerable benefit from adding preoperative therapy providing chemotherapy or CRT before the standard strategy.[5] Preoperative therapy can expand a population of patients eligible to undergo curative surgery by reducing tumors at inoperable locations. Additionally, it can obviate unnecessary surgery for patients with invisible in image, but uncontrollable metastasis.[6,7] In the speculation, preoperative irradiation may control local invasions, while preoperative chemotherapy may inhibit micrometastases. Hence, preoperative CRT can control both local invasions and micro invisible metastases and increase an effect of surgery, consequently bringing a preferable prognosis by decreasing tumor recurrences. Meanwhile, emerging evidence has suggested that, paradoxically, irradiation/chemotherapy can spare CSCs and promote malignant phenotype associating metastasis, for example, EMT in several cancers.[8–11] To avoid (or target) these paradoxical effects, we have to elucidate the molecular mechanisms underlying irradiation/chemotherapy-induced malignant abilities.

The receptor of HGF,[12] c-Met, is reported as a CSC marker in PDAC,[13,14] and PDAC tissues are known to contain abundant HGF, which is synthesized in the surrounding niche. Pancreatic ductal adenocarcinoma cells that express high c-Met

levels, which may contain abundant CSCs, are implicated in clinical CRT refractoriness and distant metastasis.[13] Therefore, we hypothesized that preoperative CRT might select specific cells, including CSCs, or stimulate high c-Met expression in PDAC cells, which might confer malignant capabilities in the remnant cells. A confirmation of this hypothesis could lead to a new therapeutic target to current CRT treatments. However, no previous study has revealed the role of c-Met expression in clinical samples or the association between c-Met expression and preoperative CRT. We here showed that c-Met expression was upregulated by CRT, and its expression was involved in the prognosis of PDAC. Moreover, we identified a transcriptional factor induced by radiation-associated miRNA. This mechanism related with c-Met expression could be a new therapeutic target in PDAC.

Materials and Methods

Patients and specimens. This study is a non-randomized single institutional retrospective analysis of c-Met using resected specimens of patients with PDAC who were enrolled in two sequential clinical trials on preoperative CRT at our institution from April 2007 to August 2012.[15,16] During this 6-year period, all eligible patients were invited to participate. We evaluated 92 patients that received R0 resections of PDAC with or without preoperative CRT. Patients were excluded from this study when they had intraductal papillary mucinous neoplasms or mucinous cystic adenocarcinomas. The clinicopathological features of these patients are shown in Table S1.

The differences between these two clinical trials are detailed in Appendix S1 (Preoperative CRT). Fifty-six patients received preoperative CRT prior to surgery (Preoperative CRT), and 36 patients underwent surgery without preoperative CRT (Non-CRT). In 2007, we began to recommend adjuvant chemotherapy after curative surgery to all patients in our institution. Gemcitabine was used in 2007–2011, and starting in 2012, S-1 (oral fluoropyrimidine anticancer drug) was typically used, according to the latest evidence from clinical trials (CONCO-001, 2007; JASPAC-001, 2011).[17,18]

Resected specimens were immediately fixed in 10% formalin for 48 h. Specimens were then embedded in paraffin and sectioned into 3.5-μm slices for further evaluations, as described previously.[19] A proportion of slides were routinely stained with H&E for pathological evaluation by certified pathologists in our institution. The remaining slides were examined with immunohistochemistry (described below).

Ethics statement on clinical samples. The use of resected samples was approved by the Human Ethics Review Committee of the Graduate School of Medicine, Osaka University (Osaka, Japan; approval number 15462). Written informed consent on usage of resected specimens was obtained from all patients.

Immunohistochemical staining. Immunohistochemical staining was carried out as previously described.[20] Briefly, paraformaldehyde-fixed, paraffin-embedded, pancreatic cancer tissue sections were deparaffinized, hydrated, and incubated with primary antibody overnight at 4°C. We used the following primary antibodies: anti-human c-Met (1:400; Santa Cruz Biotechnology, Dallas, TX, USA), anti-human ETS1 (6 μg/mL; Abcam, Cambridge, MA, USA). Bound antibodies were detected with biotin-conjugated secondary antibodies, which reacted with diaminobenzidine (Vector Laboratories, Burlingame, CA, USA), and the sections were counterstained with hematoxylin.

Semiquantitative scoring for immunohistochemistry. The expression levels of c-Met and ETS1 were evaluated with the semiquantitative scoring method, as previously described.[21] Observers blinded from all clinicopathological data used a light microscope at a magnification of 100× to grade the staining intensity of c-Met (scale, 0–2), the staining intensity of ETS1 (scale, 0–1), and the staining proportion both of c-Met and ETS1. In all cases, a higher number indicated a higher staining intensity. Reference samples (assigned an intensity of 1) were vascular smooth muscle cells for c-Met and Langerhans cells for ETS1. We identified five fields including viable cancer ducts and acquired images of representative areas. The percentage of area covered by positively stained tumor cells was calculated for each specimen. Tumor areas were assigned a proportion score that ranged from 0 to 2: 0, 0–25%; 1, 26–50%; and 2, >50%. Each intensity score was multiplied by a proportion score to obtain a final semiquantitative score. The cut-off point was set for distinguishing high expressing tumors from low expressing tumors. For 92 c-Met specimens, the cut-off score was the average score of 7; for 88 ETS1 specimens, the cut-off score was the median score of 4.

Cell lines and cell culture. Four human PDAC cell lines, MiaPaCa2, Panc1, PSN1, and BxPC3, were purchased from the Japan Cancer Research Resources Bank (Tokyo, Japan). Stable GEM-resistant cells were established by long-term exposure to GEM (Eli Lilly Pharmaceuticals, Indianapolis, IN, USA).[19,22] Three clones were derived from MiaPaCa2 (MiaPaCa2-GRs: MiaPaCa2-GR1, MiaPaCa2-GR2, and MiaPaCa2-GR3) and three clones were derived from Panc1 (Panc1-GRs: Panc1-GR1, Panc1-GR2, and Panc1-GR3). These cells were maintained as previously described.[19]

Establishment of radioresistant cell lines. The method for establishing radioresistant cell lines by fractionated irradiation was described previously.[23] First, Panc1 parent cells were passaged and seeded at 10% confluence in 100-mm tissue culture dishes (Iwaki Glass, Chiba, Japan). When cells reached 50% confluence, they were exposed to 2 Gy irradiation with a Gamma Cell 40 Exactor (Nordion International, Ottawa, ON, Canada); cells were then cultured to 90% confluence before the next passage. This radiation challenge was repeated until the total radiation dose was 60 Gy. After separating single cells with the limiting dilution method, five cell clones grew from the exposed cells (Panc1-clone1, Panc1-clone2, Panc1-clone3, Panc1-RR1, and Panc1-RR2).

Assay for radiosensitivity. As previously described,[24] cell survival after X-ray irradiation was measured in a clonogenic assay. We plated 1×10^2 cells, 2×10^2 cells, 4×10^2 cells, and 8×10^2 cells (Panc1 Parent cells, Panc1-clones, and Panc1-RRs) in separate 60-mm tissue culture dishes (Iwaki Glass). Cells were then irradiated at 0, 2, 4, and 8 Gy (three plates for each radiation dose). These cells were incubated at 37°C for 14 days. After fixation with formalin, cells were stained with 0.1% crystal violet. Colonies with more than 50 cells were counted with a light microscope, and these colony numbers were used to calculate the surviving fraction.

MicroRNA microarray experiments. MicroRNA microarray analysis was carried out by Toray Industries (Tokyo, Japan) with the TORAY 3D-Gene platform. Purified miRNAs were obtained from untreated Panc1 cells, Panc1 cells after exposure to 4 Gy irradiation, and Panc1-RR clones.

Statistical analysis. Data are expressed as the mean ± SD. Clinicopathological parameters were compared with the χ^2-test, and continuous variables were compared with Student's *t*-test. Survival curves were constructed with the

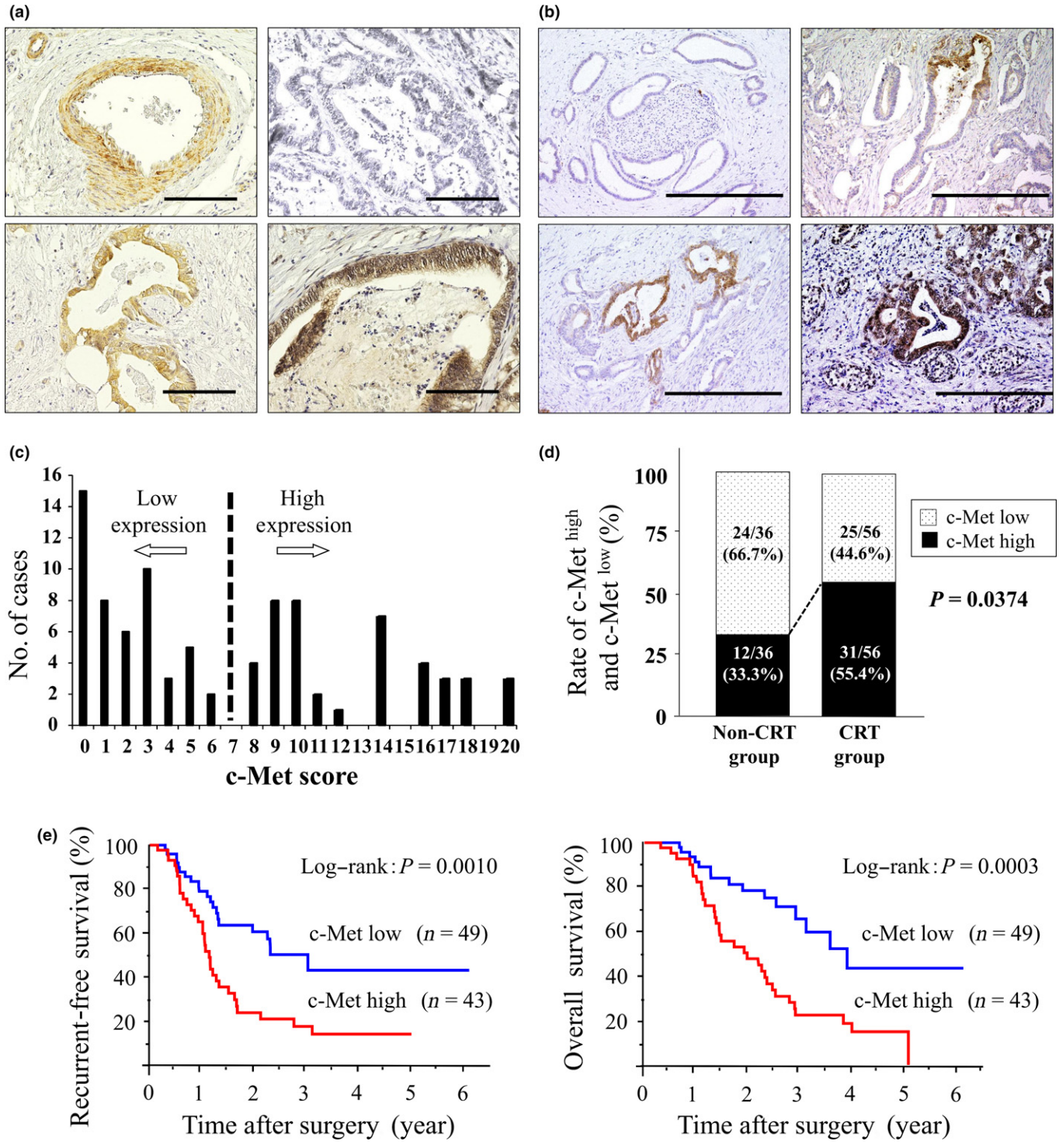

Fig. 1. Clinical impact of preoperative chemoradiation therapy (CRT) on c-Met expression in human pancreatic ductal adenocarcinoma (PDAC). (a) Representative patterns of immunohistochemical staining for c-Met about intensity; Left upper panel shows a representative pattern of vascular smooth muscle cells as reference samples assigned an intensity score 1. Representative images with each intensity score are shown for PDAC cells with c-Met negative expression assigned an intensity score 0 (right upper panel), PDAC cells with c-Met-positive expression assigned as an intensity of 1 (left bottom panel), and PDAC cells with strongly positive c-Met expression assigned as an intensity of 2 (right bottom panel). (b) Representative patterns of immunohistochemical staining for c-Met about proportion; Representative images with each proportion score are shown for PDAC cells with no area covered by positively stained tumor cells, assigned proportion score 0 (left upper panel), with 0–25% area by positively stained tumor cells, assigned proportion score 0 (right upper panel), with 25–50% area by positively stained tumor cells, assigned proportion score 1 (left bottom panel), and with >50% area by positively stained tumor cells, assigned proportion score 2 (right bottom panel). (c) Distribution of c-Met score. (d) Ratios of high to low c-Met expression in tissues from patients with PDAC that either received (CRT; $n = 56$) or did not receive (Non-CRT; $n = 36$) preoperative CRT. Preoperative CRT was significantly associated with high c-Met expression ($P = 0.0374$). (e) Kaplan–Meier analysis of patients with PDAC based on c-Met expression. The high c-Met group showed significantly shorter rates of recurrence-free and overall survival. (a, b) Scale bar = 500 μm.

Table 1. Results from univariate and multivariate analyses of overall survival in patients with pancreatic ductal adenocarcinoma

Variables (dichotomous groups)	Univariate analysis		Multivariate analysis	
	HR (95% CI)	*P*-value	HR (95% CI)	*P*-value
Age, ≥65/<65 years	1.373 (0.7635–2.551)	0.2934		
Sex, male/female	1.036 (0.5830–1.872)	0.9049		
Tumor size, ≥20/<20 mm)	2.130 (1.159–4.127)	0.0142	1.711 (0.8640–3.540)	0.1252
Tumor location, Ph/Pb or Pt	1.463 (0.8051–2.764)	0.2152		
Histopathological type, poor/well or mod	1.248 (0.2026–4.088)	0.7679		
pT, T3 or T4/T1 or T2	2.086 (1.090–4.326)	0.0256	1.423 (0.6433–3.282)	0.3882
pN, N1/N0	2.466 (1.348–4.449)	0.0038	1.888 (0.9949–3.555)	0.0518
Histologic invasion into micro tissue				
Lymph, +/–	2.115 (1.091–4.501)	0.0255	1.347 (0.6173–3.133)	0.4624
Vascular, +/–	1.520 (0.8345–2.709)	0.1674		
Nerve, +/–	1.780 (0.7722–5.160)	0.1902		
Preoperative CRT, +/–	1.084 (0.6044–1.988)	0.7885		
Adjuvant chemotherapy, +/–	0.5563 (0.2941–1.126)	0.0994		
c-Met, high/low	2.933 (1.614–5.578)	0.0003	2.952 (1.613–5.649)	0.0004

+/–, presence/absence; CI, confidence interval; CRT, chemoradiotherapy; HR, hazard ratio; mod, moderately differentiated adenocarcinoma; Pb, pancreas body; Ph, pancreas head; pN, pathological lymph node stage; poor, poorly differentiated adenocarcinoma; well, well-differentiated adenocarcinoma; Pt, pancreas tail; pT, pathological tumor stage.

Kaplan–Meier method, and differences between survival curves were compared with the log–rank test. A *P*-value ≤0.05 denoted a statistically significant difference.[25] Statistical analysis was carried out with JMP software version 11 (SAS Institute, Cary, NC, USA).

Other methods. Additional methods are described in Appendix S1.

Results

Preoperative CRT associated with high c-Met expression in PDAC. The c-Met expression score was semiquantified based on the immunohistochemistry evaluations of excised tumors (Fig. 1a,b).The distribution of c-Met score is shown in Figure 1(c). The median score of c-Met was 5, but there were two peaks in the c-Met score distribution and we chose the average score as a threshold to divide these two peaks. Based on the threshold (average) score as described above, 92 patients were divided into groups of high or low expression. Of the 92 tumors, 43 (46.7%) showed high c-Met expression. Tumor factors, such as tumor size, UICC stage, and microscopic invasions, were evaluated by the specimens. A univariate logistic analysis of canonical clinicopathological findings revealed that no tumor or patient factors affected c-Met expression, except the preoperative CRT (Fig. 1d, Table S2, $P = 0.0374$). Notably, despite the lack of a relationship between c-Met expression and tumor factors, c-Met expression was a significant prognostic marker for both recurrence-free and overall survival rates in both the univariate and multivariate analyses (Tables 1,S3, Fig. 1e). For the low and high c-Met expression groups, the median recurrence-free survival times were 27.8 and 13.8 months, respectively ($P = 0.0010$), and the median overall survival times were 46.8 and 23.7 months, respectively ($P = 0.0003$). Additionally, in the subgroup analysis, c-Met expression was a significant prognostic marker in both the CRT and non-CRT group (Fig. S1). These results revealed three new facts. First, the fraction of cancer cells that highly expressed c-Met was one of the most significant tumor factors associated with tumor progression. Second, PDAC cells that expressed c-Met were detectable even in an early stage of PDAC. Finally, preoperative CRT might increase the fraction of c-Met-expressing cancer cells present in remnant PDAC tissues.

Irradiation induced c-Met expression and activated c-Met pathways in PDAC cells. To elucidate whether a CRT-related drug or irradiation increased c-Met expression in remnant PDAC cells, we evaluated c-Met expression in GEM-resistant PDAC cells and radioresistant PDAC cells. As previously described,[19,22] with long GEM exposures, we established three independent GRs from two kinds of PDAC cell lines, MiaPaCa2 and Panc1 (Fig. S2). All the cloned cells were derived from a cell that escaped death during GEM exposure. None of these clones showed increased c-Met mRNA expression (Fig. 2a). We also established two independent radioresistant Panc1 cell clones (RR1, RR2), by cloning cells that escaped death from irradiation (Fig. 2b,c). When c-Met expression levels were evaluated in these clones, we found that the Panc1-RR clones expressed significantly higher c-Met than the parental cells, both in mRNA and protein expression assays (Fig. 2d,e). Based on these results, we concluded that the irradiation delivered in preoperative CRT increased c-Met expression in PDAC cells.

To investigate alterations in c-Met expression after radiation exposure, we measured c-Met expression levels after irradiation in four different PDAC cell lines, MiaPaCa2, Panc1, PSN1, and BxPC3. Irradiation induced elevated c-Met expression in all four PDAC cell lines (Fig. 2f), and the increase in c-Met expression was both time-dependent and dose-dependent (Fig. 2g–i, Fig. S3).

To ascertain c-Met pathway activation, the expression of canonical downstream proteins, phosphatidylinositol 3-kinase–protein kinase B,[26] MAPK,[27] signal transducer and activator of transcription,[28] and β-catenin,[29] were evaluated in MiaPaCa2 cells after irradiation. Activation of all these proteins showed both time- and dose-dependence (Fig. 2i). These results indicated that preoperative CRT could confer malignant capabilities in remnant PDAC cells through pathways involving these activated proteins.

MicroRNA-181b-5p plays a dominant role in c-Met upregulation caused by irradiation. To investigate whether epigenetic regulation played a role in the alteration of c-Met expression caused by irradiation, we undertook a comprehensive transcriptome

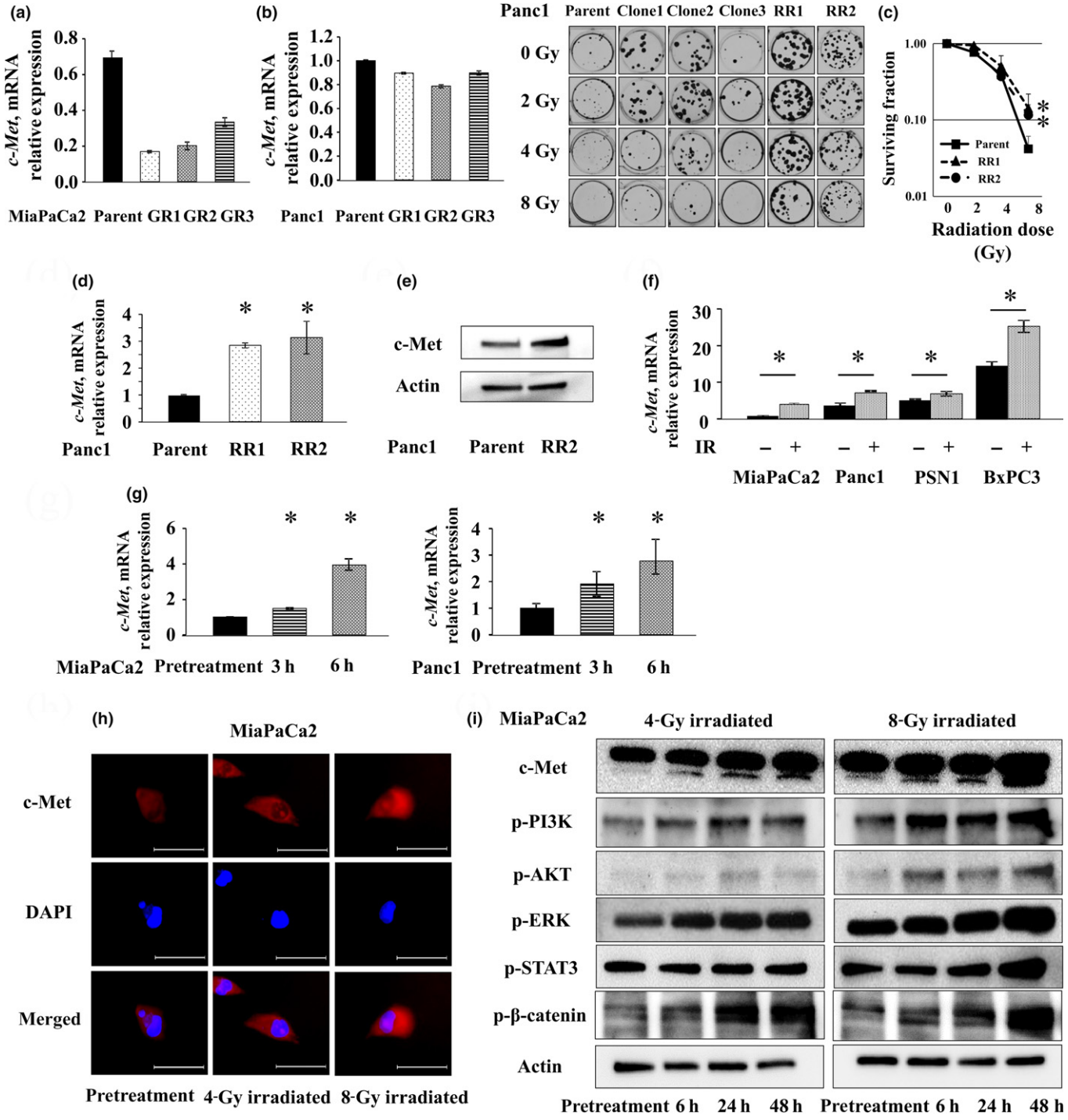

Fig. 2. c-Met expression is induced by irradiation in pancreatic ductal adenocarcinoma (PDAC) cell lines. (a) Quantitative RT-PCR results show c-Met mRNA expression did not increase in six gemcitabine-resistant cells (GR) clones (MiaPaCa2-GRs and Panc1-GRs) compared to expression in the parent cells. (b, c) Colonogenic assay for selecting radioresistant (RR) clones of Panc1. (b) Viable colonies were stained, and (c) the surviving fractions were evaluated at each radiation dose. Survival fraction = number of colonies in the dish after irradiation/the number before irradiation (0 Gy column). After a total dose of 60 Gy, only five Panc1 clones survived, and two of those clones subsequently displayed showed radioresistance by forming colonies under different irradiation doses (range, 0–8 Gy; $*P < 0.01$ *vs* Panc1 parent cells). (d) c-Met mRNA expression was significantly higher in RR cells compared parent cells. (e) Western blot analysis showed that c-Met protein expression was elevated in Panc1 RR2 cells compared to parent cells. Relative expression intensity was measured with ImageJ software. (f) c-Met mRNA expression in PDAC cell lines 6 h after exposure to 4 Gy irradiation (IR). All four cell lines showed increases in c-Met expression. (g) c-Met mRNA expression increased in both MiaPaCa2 and Panc1 cells in a time-dependent manner after exposure to 4 Gy irradiation. (h) Immunocytochemistry shows increases in c-Met expression in MiaPaCa2 cells at 48 h after exposure to the indicated irradiation. (i) Western blot analysis of whole cell lysate from MiaPaCa2 cells shows increases in c-Met protein expression. These increases showed both time dependence and dose dependence; canonical downstream signaling molecules were also activated with irradiation. Values represent the mean ± SD. $*P < 0.01$. Scale bar = 50 μm. All experiments were carried out at least three times. AKT, protein kinase B; PI3K, phospho inositide 3-kinase STAT3, signal transducer and activator of transcription 3.

Table 2. Candidate microRNAs (miR) for altering c-Met expression in Panc1 pancreatic ductal adenocarcinoma cells, based on microarray analysis

Name	Fold change *versus* non-irradiated or parental cells		
	4-Gy IR	RR1	RR2
has-miR-15a-5p	0.65	0.54	0.30
has-miR-19a-3p	0.68	0.58	0.39
has-miR-23a-3p	0.68	0.49	0.65
has-miR-25-3p	0.64	0.64	0.43
has-miR-26a-5p	0.70	0.42	0.45
has-miR-26b-5p	0.67	0.56	0.33
has-miR-29a-3p	0.70	0.60	0.54
has-miR-30a-3p	0.65	0.64	0.48
has-miR-30b-5p	0.66	0.43	0.43
has-miR-30e-3p	0.61	0.67	0.57
has-miR-31-5p	0.69	0.51	0.32
has-miR-93-5p	0.68	0.55	0.41
has-miR-100-5p	0.68	0.55	0.26
has-miR-106b-5p	0.65	0.68	0.70
has-miR-126-3p	0.60	0.59	0.43
has-miR-149-5p	0.69	0.31	0.61
has-miR-151b	0.68	0.53	0.52
has-miR-181b-5p	0.67	0.64	0.56
has-miR-185-5p	0.70	0.59	0.47
has-miR-222-5p	0.49	0.40	0.24
has-miR-224-5p	0.70	0.39	0.42
has-miR-320c	0.66	0.47	0.64
has-miR-320d	0.66	0.53	0.61
has-miR-361	0.61	0.68	0.58
has-miR-378a-3p	0.65	0.65	0.64
has-miR-422a	0.60	0.63	0.65
has-miR-574-5p	0.69	0.69	0.68
has-miR-2278	0.36	0.61	0.70
has-miR-3151-3p	0.51	0.63	0.34
has-miR-4291	0.69	0.57	0.64
has-miR-4443	0.70	0.70	0.44
has-miR-4738-3p	0.58	0.65	0.44
has-miR-5685	0.63	0.60	0.37
has-miR-6742-3p	0.65	0.57	0.65
has-miR-6848-3p	0.35	0.68	0.61
has-miR-7114-3p	0.66	0.63	0.63
let-7c-5p	0.63	0.52	0.44
let-7d-5p	0.69	0.53	0.46
let-7 g-5p	0.70	0.56	0.43
let-7i-5p	0.65	0.63	0.38

IR, irradiated; RR, radioresistant cell clone.

analysis, which included miRNAs. We compared miRNA expression levels between irradiated Panc1 cells and non-irradiated Panc1 cells, and between two different radioresistant Panc1 clones and parental Panc1 cells. Among the 2565 miRNAs identified, we first focused on the downregulated miRNAs (threshold was set under 0.7-fold). We found 40 candidate miRNAs that overlapped in all the comparisons (Table 2); among these, the prediction algorithm, TargetScan (http://www.targetscan.org/vert_71/), revealed that *miR-181b-5p* was the only gene that could involve c-Met expression. We confirmed that radiation induced miR-181b-5p downregulation, based on similar observations in MiaPaCa2 cells exposed to irradiation (Fig. 3a). Furthermore, when pre-miR-181b-5p was overexpressed in MiaPaCa2 cells (Fig. S4), we found no increase in c-Met and p-Met expression, even after irradiation (Fig. S5). These results indicated that the downregulation of miR-181b-5p played a dominant role in c-Met expression after radiation exposure (Fig. 3b,c).

c-Met upregulation by ETS1 activation, following miR-181b-5p inhibition. The v-ets avian erythroblastosis virus E26 oncogene homolog 1 (ETS1) is a transcription factor that controls some invasive growth genes.[30] ETS1 was shown to bind to the *MET* promoter, which activated *MET* transcription *in vitro*.[31] Moreover, because mir-181b-5p targeted the *ETS1* gene, we expected that ETS1 expression would be affected by miR-181b-5p expression. We found that irradiation increased the levels of nuclear ETS1, which indicated activated *ETS1* expression. This radiation effect was both time-dependent and dose-dependent (Fig. 3d,e). As expected, the transduction of pre-miR-181b-5p into PDAC cells inhibited ETS1 expression, even after irradiation (Fig. 3f–h). Moreover, similar results were found when we knocked down ETS1 mRNA with siRNAs specific for ETS1 (si*ETS1*). MiaPaCa2 cells transduced with si*ETS1* showed no increase in c-Met expression after irradiation (Fig. 3i–k). These results revealed that ETS1 was a target of miR-181b-5p, and ETS1 was a dominant factor in c-Met upregulation caused by irradiation.

Immunohistochemical assessment of ETS1 expression in primary PDAC samples. To validate the mechanism that c-Met expression was upregulated by an increase in ETS1 after irradiation, we carried out immunohistochemical staining for ETS1 in clinical specimens (Fig. 4a,b). Of the 88 tumors, 44 (50.0%) showed high ETS1 expression. A univariate analysis of associations between clinicopathological background characteristics and ETS1 expression revealed that the only factor that affected ETS1 expression in resected PDAC tissues was the presence of preoperative CRT (Table 3, $P = 0.0043$), similar to the results from the univariate analysis of c-Met expression. Moreover, high c-Met expression was significantly associated with high ETS1 expression (Table 3, $P = 0.0025$). Both c-Met and ETS1 expressions were detected in the same cancer cells with using serial section of specimen (Fig. 4c). These results indicated that ETS1 expression was significantly correlated with c-Met expression in clinical samples. These results were consistent with our findings *in vitro*.

Discussion

This basic study revealed three new findings. First, patients with high c-Met expression showed a distinctly shorter survival time than those with low c-Met expression. Second, c-Met expression in PDAC was significantly associated with the presence of preoperative CRT. Finally, radiation exposure induced c-Met expression in PDAC cells by inhibiting miR-181b-5p, which released its suppression of the transcription factor, ETS1; in turn, increased ETS1 levels enhanced c-Met transcription.

Recently, two oncological mechanisms, the EMT and the presence of CSCs were reported to be associated with resistance to chemo-/irradiation therapy in various cancers.[9–11] Previous reports showed that HGF could induce EMT in PDAC cells; moreover, the HGF receptor, c-Met, was identified as a dominant pancreatic CSC marker.[14] Therefore, it was expected that c-Met expression of PDAC can be a prognostic marker despite no report assuming that, and actually, c-Met expression was previously identified as an indicator of poor prognosis in various cancers,[32,33] and a c-Met inhibitor was developed as a

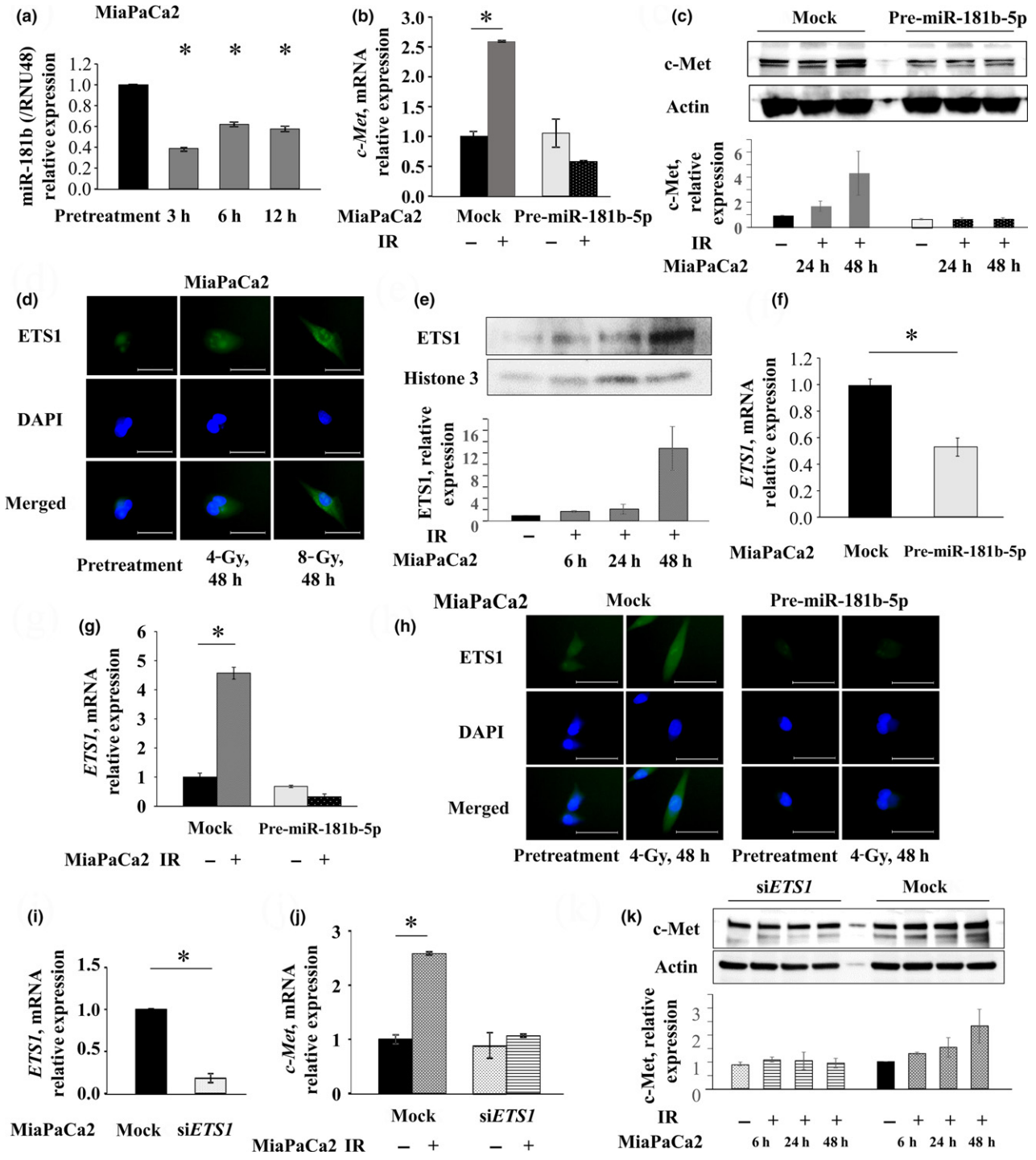

Fig. 3. Mechanism underlying c-Met induction by radiation exposure. (a) Quantitative RT-PCR results show changes in c-Met mRNA expression at different time points after exposure to 4 Gy irradiation. Radiation suppressed miR-181b expression in MiaPaCa2 cells. (b, c) Pre-microRNA (miR)-181b was overexpressed in MiaPaCa2 cells. (b, c) Quantitative RT-PCR (b) and Western blot results (c) show that, in the presence of high miR-181b-5p levels, c-Met mRNA expression did not increase after exposure to 4 Gy irradiation (IR). (d) Immunocytochemistry images show that ETS1 protein expression increased in nuclei after exposure to irradiation in MiaPaCa2 cells. (e) Western blot of nuclear proteins extracted from MiaPaCa2 cells shows that ETS1 expression was induced by 4-Gy IR in a time-dependent manner. The relative expression intensity was measured with ImageJ software (https://imagej.nih.gov/ij/). (f, g) ETS1 mRNA expression in the presence or absence of pre-miR-181b-5p overexpression in MiaPaCa2 cells. Overexpression of pre-miR-181b-5p significantly inhibited ETS1 expression (f), even after exposure to 4 Gy IR (g). (h) Immunocytochemistry images of ETS1 expression in MiaPaCa2 cells before and after exposure to 4 Gy irradiation. Transduction of pre-miR-181b-5p inhibited ETS1 expression, even after 4 Gy irradiation. (i) ETS1 mRNA expression was knocked down in MiaPaCa2 cells with transduction of si*ETS1*. (j) si*ETS1* knockdown attenuated the increase in c-Met mRNA observed at 6 h after exposure to 4 Gy IR. (k) Top, Western blot of whole cell lysate from MiaPaCa2 cells transfected with or without si*ETS1*, measured at 48 h after 4 Gy IR. Bottom, c-Met expression levels were evaluated 6, 24, and 48 h after exposure to 4 Gy IR. Relative expression intensity was measured with ImageJ software. c-Met protein expression was not increased after irradiation when ETS1 was knocked down in MiaPaCa2 cells. Values represent mean ± SD. $*P < 0.01$. Scale bar = 50 μm. All experiments were carried out at least three times.

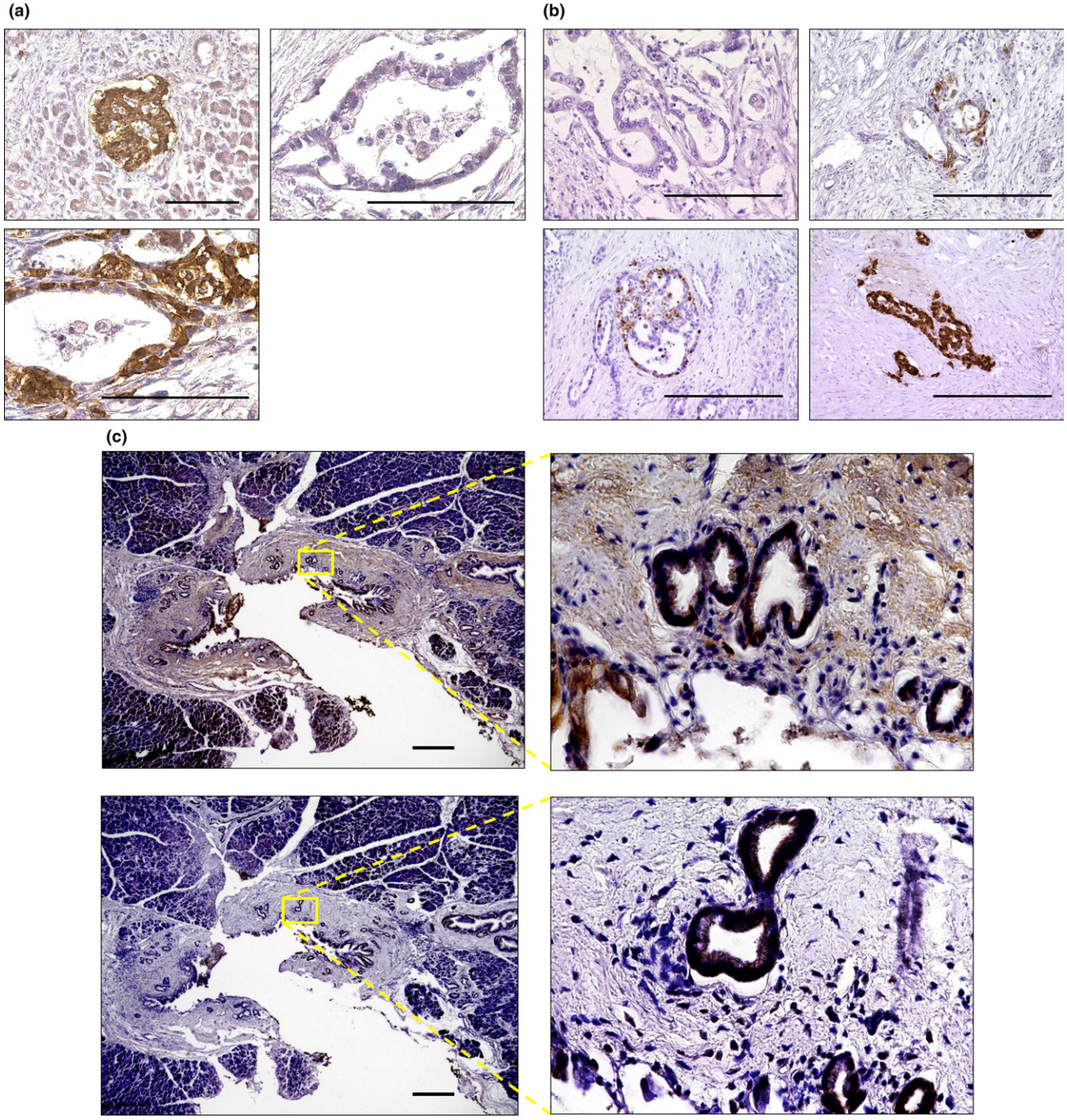

Fig. 4. Clinical impact of preoperative chemoradiation therapy (CRT) on ETS1 expression in human clinical samples of pancreatic ductal adenocarcinoma (PDAC) tissues. (a) Representative patterns of immunohistochemical staining for ETS1 intensity. Left upper panel, representative patterns of Langerhans cells as reference samples assigned intensity score 1. Representative images with each intensity score are shown for PDAC cells with ETS1 negative expression assigned intensity score 0 (right upper panel), PDAC cells with ETS1 positive expression assigned as intensity of 1 (left bottom panel). Scale bar = 500 μm. (b) Representative patterns of immunohistochemical staining for ETS1 about proportion. Representative images with each proportion score are shown for PDAC cells with no area covered by positively stained tumor cells assigned proportion score 0 (left upper panel), with 0–25% area by positively stained tumor cells assigned proportion score 0 (right upper panel), with 25–50% area by positively stained tumor cells assigned proportion score 1 (left bottom panel), and with >50% area by positively stained tumor cells assigned proportion score 2 (right bottom panel). Scale bar = 500 μm. (c) Representative patterns of immunohistochemical staining for ETS1 and c-Met in a serial section. Left upper panel, representative pattern of PDAC cells with ETS1 positive expression (×40). Right upper panel, enlarged image. Left bottom panel, representative pattern of PDAC cells with c-Met-positive expression (×40). Right bottom panel, enlarged image. Scale bar = 50 μm.

candidate drug for treating advanced hepatocellular carcinoma.[34] Our results firstly elucidated the role of c-Met expression in PDAC. We found that c-Met was significantly associated with both recurrent-free and overall survival time.

During the last decade, preoperative CRT for PDAC has emerged as a reasonable strategy.[5,6,35] But the efficacy of preoperative CRT on the control of distant metastasis, especially liver metastasis, remains unclear, and there is scarce evidence

Table 3. Clinicopathological factors in patients with pancreatic ductal adenocarcinoma, stratified by level of ETS1 expression

Characteristics (dichotomous groups)	ETS1 expression (number of patients)		*P*-value
	High (n = 44)	Low (n = 44)	
Age, <65:≥65 years	18:26	16:28	0.6614
Sex, male: female	27:17	26:18	0.8276
Tumor size, <20:≥20 mm	21:23	14:30	0.1264
Histopathological type, well or mod: poor	43:1	41:3	0.2956
cT, 1 or 2:3 or 4	7:37	11:33	0.2888
pT, 1 or 2:3 or 4	12:32	13:31	0.8131
pN, 0:1	29:15	27:17	0.6575
pStage, IA or IB or IIA:IIB or III or IV	29:15	27:17	0.6575
Histologic invasion into micro tissue			
Lymph, −:+	15:29	13:31	0.6470
Vascular, −:+	30:14	27:17	0.5029
Nerve, −:+	9:35	10:34	0.7955
Preoperative CRT, −:+	11:33	24:20	0.0043
c-Met, low:high	17:27	31:13	0.0025

+:−, presence or absence; CRT, chemoradiotherapy; cT, clinical tumor stage; mod, moderately differentiated adenocarcinoma; poor, poorly differentiated adenocarcinoma; pN, pathological lymph node stage; pStage, pathological stage defined by UICC classification (version 6); pT, pathological tumor stage; well, well-differentiated adenocarcinoma.

that preoperative CRT is superior to preoperative chemotherapy for all PDAC patients. In this study, c-Met expression in resected specimens of PDAC was significantly associated with the presence of preoperative CRT. In addition, when PDAC cells were irradiated, remnant cells showed c-Met upregulation and an activation of a canonical pathway downstream of HGF/c-Met. A previous report suggested that irradiation could increase c-Met expression in some pancreatic cancer cell lines *in vitro*,[36] and our results were compatible. The activation of c-Met following HGF binding resulted in invasive growth and induced EMT in various cancer cells, including PDAC.[37] Because overactivation of c-Met, followed by activation of downstream signal transducer molecules, protein kinase B, ERK, and signal transducer and activator of transcription 3, promoted the ability of invasion or metastasis,[28,29,38] our results indicated that high c-Met expression induced by irradiation could promote malignant traits in PDAC cells. Thus, radiation therapy could have two aspects; one is a benefit of enhancing local control, and the other is a side-effect of promoting malignant potentials in remnant PDAC cells. Our findings may suggest that irradiation therapy does not benefit all PDAC patients; however, especially in the cases of borderline resectable PDAC, preoperative CRT could have a strong impact in downstaging. Hence, we should not omit this procedure in certain patients and must explore the mechanisms involved in c-Met elevation with irradiation. We undertook further investigation to reveal the mechanisms.

The present study revealed three new insights regarding c-Met upregulation. First, an irradiation-induced inhibition of miR-181b-5p expression was associated with ETS1 upregulation. Second, there are four ETS family binding sites in the *MET* promoter;[30,31] therefore, it is reasonable to assume that ETS1 upregulation directly increased c-Met expression in PDAC cells. Finally, c-Met mRNA expression was not increased by long-term exposure to GEM.

MicroRNA-181b-5p was reported to antagonize apoptosis. Its target genes were reported to be NOVA1, Narp, and Notch.[39,40] Although *ETS1* was not previously identified as a target gene of miR-181b-5p, the prediction algorithm, TargetScan, indicated that miR-181b-5p could target conserved sites located in the 3′-UTR of ETS1. Accordingly, in the present study, our results indicated that ETS1 was a target of miR-181b-5p.

In recent years, ETS1 has gained attention in cancer research, due to its importance in cell migration, invasion, and proliferation, which suggested that it could be involved in EMT.[41] Our present results were consistent with those previous reports. Our retrospective analysis of clinical samples revealed that c-Met expression was an independent prognostic factor; it showed a strong, positive interaction with preoperative CRT and with ETS1 expression.

In summary, we found that c-Met expression was involved in the overall survival of patients with PDAC. Irradiation downregulated miR-181b-5p, which released suppression of ETS1 expression. The increase in ETS1 expression caused an upregulation of c-Met expression. Our findings suggested that applying a c-Met inhibitor during preoperative CRT may be an optimal strategy in PDAC, because it might inhibit distant recurrences after curative surgery.

Acknowledgments

We thank the members of our laboratory for technical advice and helpful discussion. This work was supported in part by a grant from the Osaka Cancer Society and in part by a grant from the Pancreas Research Foundation of Japan.

Disclosure Statement

The authors have no conflict of interest.

Abbreviations

CRT	chemoradiation therapy
CSC	cancer stem cell
EMT	epithelial–mesenchymal transition
ETS1	v-ets avian erythroblastosis virus E26 oncogene homolog 1
GEM	gemcitabine
GR	gemcitabine-resistant clone
HGF	hepatocyte growth factor
miRNA	microRNA
PDAC	pancreatic ductal adenocarcinoma
RR	radioresistant cell clone

References

1 Raju RS, Coburn N, Liu N *et al.* A population-based study of the epidemiology of pancreatic cancer: a brief report. *Curr Oncol* 2015; **22**: e478–84.
2 Siegel RL, Miller KD, Jemal A. Cancer statistics, 2016. *CA Cancer J Clin* 2016; **66**: 7–30.
3 Siegel R, Naishadham D, Jemal A. Cancer statistics for Hispanics/Latinos, 2012. *CA Cancer J Clin* 2012; **62**: 283–98.

4 Oettle H, Neuhaus P, Hochhaus A *et al.* Adjuvant chemotherapy with gemcitabine and long-term outcomes among patients with resected pancreatic cancer: the CONKO-001 randomized trial. *JAMA* 2013; **310**: 1473–81.
5 Evans DB, Varadhachary GR, Crane CH *et al.* Preoperative gemcitabine-based chemoradiation for patients with resectable adenocarcinoma of the pancreatic head. *J Clin Oncol* 2008; **26**: 3496–502.
6 Gillen S, Schuster T, Meyer Zum Buschenfelde C, Friess H, Kleeff J. Preoperative/neoadjuvant therapy in pancreatic cancer: a systematic review and meta-analysis of response and resection percentages. *PLoS Med* 2010; **7**: e1000267.
7 Morganti AG, Massaccesi M, La Torre G *et al.* A systematic review of resectability and survival after concurrent chemoradiation in primarily unresectable pancreatic cancer. *Ann Surg Oncol* 2010; **17**: 194–205.
8 Cui YH, Suh Y, Lee HJ *et al.* Radiation promotes invasiveness of non-small-cell lung cancer cells through granulocyte-colony-stimulating factor. *Oncogene* 2015; **34**: 5372–82.
9 Kawamoto A, Yokoe T, Tanaka K *et al.* Radiation induces epithelial-mesenchymal transition in colorectal cancer cells. *Oncol Rep* 2012; **27**: 51–7.
10 Yan S, Wang Y, Yang Q *et al.* Low-dose radiation-induced epithelial-mesenchymal transition through NF-kappaB in cervical cancer cells. *Int J Oncol* 2013; **42**: 1801–6.
11 Doherty MR, Smigiel JM, Junk DJ, Jackson MW. Cancer stem cell plasticity drives therapeutic resistance. *Cancers* 2016; **8**. doi: 10.3390/cancers8010008.
12 Bottaro DP, Rubin JS, Faletto DL *et al.* Identification of the hepatocyte growth factor receptor as the c-met proto-oncogene product. *Science (New York, NY)* 1991; **251**: 802–4.
13 Hermann PC, Huber SL, Herrler T *et al.* Distinct populations of cancer stem cells determine tumor growth and metastatic activity in human pancreatic cancer. *Cell Stem Cell* 2007; **1**: 313–23.
14 Li C, Wu JJ, Hynes M *et al.* c-Met is a marker of pancreatic cancer stem cells and therapeutic target. *Gastroenterology* 2011; **141**: 2218–27.e5.
15 Eguchi H, Nagano H, Tanemura M *et al.* Preoperative chemoradiotherapy, surgery and adjuvant therapy for resectable pancreatic cancer. *Hepatogastroenterology* 2013; **60**: 904–11.
16 Eguchi H, Nagano H, Kobayashi S *et al.* A phase I trial of combination therapy using gemcitabine and S-1 concurrent with full-dose radiation for resectable pancreatic cancer. *Cancer Chemother Pharmacol* 2014; **73**: 309–15.
17 Oettle H, Post S, Neuhaus P *et al.* Adjuvant chemotherapy with gemcitabine vs observation in patients undergoing curative-intent resection of pancreatic cancer: a randomized controlled trial. *JAMA* 2007; **297**: 267–77.
18 Maeda A, Boku N, Fukutomi A *et al.* Randomized phase III trial of adjuvant chemotherapy with gemcitabine versus S-1 in patients with resected pancreatic cancer: Japan Adjuvant Study Group of Pancreatic Cancer (JASPAC-01). *Jpn J Clin Oncol* 2008; **38**: 227–9.
19 Iwagami Y, Eguchi H, Nagano H *et al.* miR-320c regulates gemcitabine-resistance in pancreatic cancer via SMARCC1. *Br J Cancer* 2013; **109**: 502–11.
20 Kondo M, Yamamoto H, Nagano H *et al.* Increased expression of COX-2 in nontumor liver tissue is associated with shorter disease-free survival in patients with hepatocellular carcinoma. *Clin Cancer Res* 1999; **5**: 4005–12.
21 Olaussen KA, Dunant A, Fouret P *et al.* DNA repair by ERCC1 in non-small-cell lung cancer and cisplatin-based adjuvant chemotherapy. *N Engl J Med* 2006; **355**: 983–91.
22 Hasegawa S, Eguchi H, Nagano H *et al.* MicroRNA-1246 expression associated with CCNG2-mediated chemoresistance and stemness in pancreatic cancer. *Br J Cancer* 2014; **111**: 1572–80.
23 Matsuyama A, Inoue H, Shibuta K *et al.* Hepatoma-derived growth factor is associated with reduced sensitivity to irradiation in esophageal cancer. *Cancer Res* 2001; **61**: 5714–7.
24 Franken NA, Rodermond HM, Stap J, Haveman J, van Bree C. Clonogenic assay of cells in vitro. *Nat Protoc* 2006; **1**: 2315–9.
25 Izumi S, Nakamura S, Mano S, Onoda Y. Well-differentiated pancreatic ductal adenocarcinomas measuring ≤ 1 cm exhibit early features of tumor progression: a report of five lesions and a comparative study with advanced lesions. *Surg Today* 2014; **44**: 2058–64.
26 Gentile A, Trusolino L, Comoglio PM. The Met tyrosine kinase receptor in development and cancer. *Cancer Metastasis Rev* 2008; **27**: 85–94.
27 O'Brien LE, Tang K, Kats ES, Schutz-Geschwender A, Lipschutz JH, Mostov KE. ERK and MMPs sequentially regulate distinct stages of epithelial tubule development. *Dev Cell* 2004; **7**: 21–32.
28 Boccaccio C, Ando M, Tamagnone L *et al.* Induction of epithelial tubules by growth factor HGF depends on the STAT pathway. *Nature* 1998; **391**: 285–8.
29 Monga SP, Mars WM, Pediaditakis P *et al.* Hepatocyte growth factor induces Wnt-independent nuclear translocation of beta-catenin after Met-beta-catenin dissociation in hepatocytes. *Cancer Res* 2002; **62**: 2064–71.
30 Shirasaki F, Makhluf HA, LeRoy C, Watson DK, Trojanowska M. Ets transcription factors cooperate with Sp1 to activate the human tenascin-C promoter. *Oncogene* 1999; **18**: 7755–64.
31 Gambarotta G, Boccaccio C, Giordano S, Ando M, Stella MC, Comoglio PM. Ets up-regulates MET transcription. *Oncogene* 1996; **13**: 1911–7.
32 Shoji H, Yamada Y, Taniguchi H *et al.* Clinical impact of c-MET expression and genetic mutational status in colorectal cancer patients after liver resection. *Cancer Sci* 2014; **105**: 1002–7.
33 Lv H, Shan B, Tian Z, Li Y, Zhang Y, Wen S. Soluble c-Met is a reliable and sensitive marker to detect c-Met expression level in lung cancer. *BioMed Res Int* 2015; **2015**: 626578.
34 Qi XS, Guo XZ, Han GH, Li HY, Chen J. MET inhibitors for treatment of advanced hepatocellular carcinoma: a review. *World J Gastroenterol* 2015; **21**: 5445–53.
35 Paulson AS, Tran Cao HS, Tempero MA, Lowy AM. Therapeutic advances in pancreatic cancer. *Gastroenterology* 2013; **144**: 1316–26.
36 Qian LW, Mizumoto K, Inadome N *et al.* Radiation stimulates HGF receptor/c-Met expression that leads to amplifying cellular response to HGF stimulation via upregulated receptor tyrosine phosphorylation and MAP kinase activity in pancreatic cancer cells. *Int J Cancer* 2003; **104**: 542–9.
37 Peruzzi B, Bottaro DP. Targeting the c-Met signaling pathway in cancer. *Clin Cancer Res* 2006; **12**: 3657–60.
38 Bean J, Brennan C, Shih JY *et al.* MET amplification occurs with or without T790M mutations in EGFR mutant lung tumors with acquired resistance to gefitinib or erlotinib. *Proc Natl Acad Sci USA* 2007; **104**: 20932–7.
39 Zhi F, Wang Q, Deng D *et al.* MiR-181b-5p downregulates NOVA1 to suppress proliferation, migration and invasion and promote apoptosis in astrocytoma. *PLoS One* 2014; **9**: e109124.
40 Zhang C, Hou D, Feng X. Mir-181b functions as anti-apoptotic gene in post-status epilepticus via modulation of Nrarp and Notch signaling pathway. *Ann Clin Lab Sci* 2015; **45**: 550–5.
41 Li C, Wang Z, Chen Y *et al.* Transcriptional silencing of ETS-1 abrogates epithelial-mesenchymal transition resulting in reduced motility of pancreatic cancer cells. *Oncol Rep* 2015; **33**: 559–65.

Supporting Information

Additional Supporting Information may be found online in the supporting information tab for this article:

Appendix S1. Materials and methods.

Fig. S1. Kaplan–Meier analysis of patients with pancreatic ductal adenocarcinoma based on c-Met expression in the non-chemoradiation group and chemoradiation group.

Fig. S2. Verification of resistances to gemcitabine in the gemcitabine-resistance clones.

Fig. S3. c-Met expression is induced by irradiation in pancreatic ductal adenocarcinoma cell lines.

Fig. S4. Transduction with pre-miR-181b-5p in MiaPaCa2 pancreatic ductal adenocarcinoma cells.

Fig. S5. Phosphatized c-Met expressions (p-Met) in MiaPaCa2 cells with or without pre-miR-181b-5p introduction.

Table S1. Clinicopathological characteristics of 92 participating patients with pancreatic ductal adenocarcinoma.

Table S2. Clinicopathological factors in patients with pancreatic ductal adenocarcinoma, stratified by the level of tumor c-Met expression.

Table S3. Results from univariate and multivariate analyses of recurrent-free survival in patients with pancreatic ductal adenocarcinoma.